Acoust. Sci. & Tech. **44**, 3 (2023)

INVITED PAPER

Models of musical string vibration

Stefan Bilbao[1,*] and Michele Ducceschi[2]

[1]*Acoustics and Audio Group, Reid School of Music, University of Edinburgh, United Kingdom*
[2]*Department of Industrial Engineering, University of Bologna, Italy*

(*Received 23 March 2022, Accepted for publication 2 December 2022*)

Abstract: Musical string vibration has been the subject of scientific study for centuries. Recent increases in computational power have allowed the exploration of increasingly detailed features of perceptual significance through simulation approaches. The starting point for any simulation is a well-defined model, usually framed as a system of differential equations, with parameters determined by measurement and experiment. This review article is intended to take the reader through models of string vibration progressively, beginning with well-known and well-studied linear models, and then introducing new features that form the basis for the modern study of realistic musical string vibration. These include, first, nonlinear excitation mechanisms, such as the hammer-string and bow-string interaction, and then the collision mechanism, both for pointwise obstructions and over a distributed region. Finally, the linear model of string vibration is generalized to include geometric nonlinear effects, leading to typical nonlinear behaviour such as pitch glides and the appearance of so-called phantom partials due to nonlinear mixing of modes. The article concludes with a general overview of numerical simulation techniques for string vibration.

Keywords: String vibration, Collision modeling, Musical acoustics

1. INTRODUCTION

The vibration of a string is the basic sound production mechanism, or resonator, at the heart of many musical instruments, far too numerous to list here. Stringed instruments have been built and played over thousands of years, and in virtually all regions of the world. See [1–4] for an overview. Modern research into musical string vibration has a shorter (but still long) history, dating back to the work of Helmholtz [5] and later Raman [6], Friedlander [7], Keller [8] and others on bowed strings.

More recently, the field has been invigorated by increases in computational power, allowing the exploration of increasingly subtle audible features of musical string vibration through simulation. Early computer simulation work in the context of sound synthesis in the late 1960s and early 1970s [9–11] was followed, over the next 25 years, by the investigation of progressively more sophisticated models of linear string vibration [12–16]. The focus broadened to include the problem of the hammer string interaction, with work continuing apace on bowed string dynamics [17–19], now including computer simulation approaches [20]. Since approximately 2000, the scope has further widened to include the modeling of strong nonlinearities, of both geometric type and due to unilateral constraints (collisions) that occur in musical instruments under playing conditions. Such developments have been due in part to the need to validate experimental results, but also because of the possibilities for greatly increased realism in synthetically-produced sound.

This review article is intended as a survey of the state of the art in musical string models. The point of view taken here is model-based rather than experimental or perceptual, following from the interests of the authors in simulation. A well-defined model, framed in terms of a set of differential equations, is the starting point for any computer simulation, and it is hoped that through a presentation of the many variants in a compact manner, readers will get a unified picture of the dynamics of musical strings, particularly if simulation is their goal.

Models of linear string vibration, beginning with the simple one-dimensional wave equation, and progressively adding effects of stiffness and loss, are covered in Sect. 2. In Sect. 3, point-like excitation models, including the bowed string and hammer are introduced, as well as a model of both pointwise and distributed unilateral constraints on string vibration. In Sect. 4, the inherent geometric nonlinearity of strings vibrating at high amplitudes, as well as the resulting perceptual effects are explored, first

*e-mail: sbilbao@ed.ac.uk
[doi:10.1250/ast.44.194]

through the simple Kirchhoff-Carrier model, and then through a complete model involving coupling between transverse and longitudinal string motion. In Sect. 5, some very rudimentary aspects of numerical simulation techniques for string vibration are discussed. Some concluding remarks and perspectives appear in Sect. 6.

2. LINEAR STRING VIBRATION

Many (but not all) features of string vibration are captured by a linear model, usually framed in terms of pure transverse motion in a single polarisation. This includes representations of the solution in terms of traveling waves, as well as the key concept of the modal frequency, which is related to the perceptual attribute of pitch.

2.1. The One-dimensional Wave Equation

The simplest possible model of the transverse vibration of the string is given by the one-dimensional wave equation:

$$\rho A \partial_t^2 u - T \partial_x^2 u = 0. \tag{1}$$

Here, $u(x,t)$ is the transverse displacement of the string, as a function of spatial coordinate $x \in \mathcal{D} \subset \mathbb{R}$, and time $t \geq 0$, in s. (Here, for analysis purposes, the spatial domain $\mathcal{D}$ is left unspecified, but ultimately it will be limited to a finite interval $\mathcal{D} = [0, L]$, for some string length L in m.) See Fig. 1. ∂_t and ∂_x represent partial differentiation with respect to t and x, respectively. Three constants appear in (1): the material density ρ, in kg·m^{-3}; the string cross sectional area A, in m^2 (set equal to πr^2, for a string of circular cross section and radius r m); and the nominal string tension T, in N. The wave equation (1) is usually written in terms of the consolidated parameter $c = \sqrt{T/\rho A}$, referred to as the wave speed. The derivation of the one-dimensional wave equation for the string appears in many texts. See, e.g., [21].

The wave equation, as given in (1) is a second order (in time) partial differential equation, and two initial conditions must be supplied:

$$u(x,0) = u_0(x) \quad \partial_t u|_{x,t=0} = v_0(x) \tag{2}$$

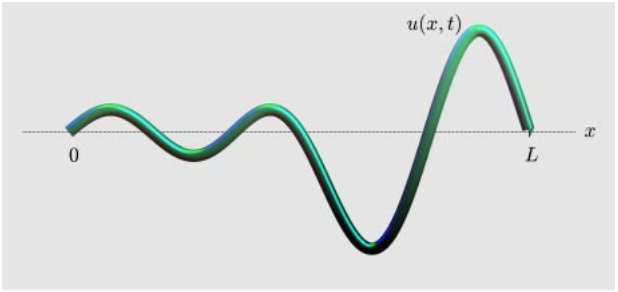

Fig. 1 Transverse displacement $u(x,t)$ of a string over the interval $x \in [0, L]$.

Here, $u_0(x)$ and $v_0(x)$ are two distributions representing the initial displacement and transverse velocity of the string respectively. Initialisation is useful for analysis purposes, but in any musical setting, the string is set into motion through external forcing, and thus initial conditions may be set to zero. See Sect. 3.

2.1.1. Dispersion relation and traveling wave solution

It is useful to examine the wave equation first in the case of an infinitely long domain, so that $\mathcal{D} = \mathbb{R}$. As a shortcut to full Fourier transform analysis, one may examine the behaviour of a monochromatic wave-like solution of the form

$$u(x,t) = \hat{u} e^{j(\omega t - kx)} \tag{3}$$

for some non-zero amplitude $\hat{u}$. Here, ω is an angular frequency, in rad.·s^{-1}, and k is a wavenumber, in m^{-1}. Insertion of this solution into (1) leads to the following dispersion relation:

$$\omega = \pm ck \tag{4}$$

and the phase velocity for such waves is:

$$v_\phi = \frac{\omega}{k} = \pm c. \tag{5}$$

Thus all waves travel to the left and right at the same speed c.

Given that this is true for a wave at any frequency ω and wavenumber k, it must also be true for a general solution. The famous d'Alembert solution [22] to the one-dimensional wave equation may be written in terms of the propagation of aribitrary distributions $u_+(x)$ and $u_-(x)$:

$$u(x,t) = u_+(x - ct) + u_-(x + ct). \tag{6}$$

u_+ and u_- may themselves be written in terms of the initial distributions $u_0(x)$ and $v_0(x)$ from (2) See Fig. 2. The traveling wave solution above forms the basis for digital waveguide approaches to string simulation [23].

2.1.2. Boundary conditions and modes

The wave equation (1) is of second order in space, and thus two boundary conditions are required—one at each end of the domain $x \in [0, L]$. The natural choice, if the string is to be examined in isolation, is fixed terminations:

$$u(0,t) = u(L,t) = 0 \quad \forall t \geq 0. \tag{7}$$

Under these conditions, and using the modal basis functions $\phi_p = \sqrt{2/L} \sin(p\pi x/L)$, for $p = 1, \ldots$ a complete solution to (1) follows as

$$u(x,t) = \sum_{p=1}^{\infty} A_p \cos(2\pi f_p t + \theta_p) \phi_p(x) \tag{8}$$

for constants A_p and θ_p that can be determined from the initial conditions (2), and at modal frequencies f_p, defined by

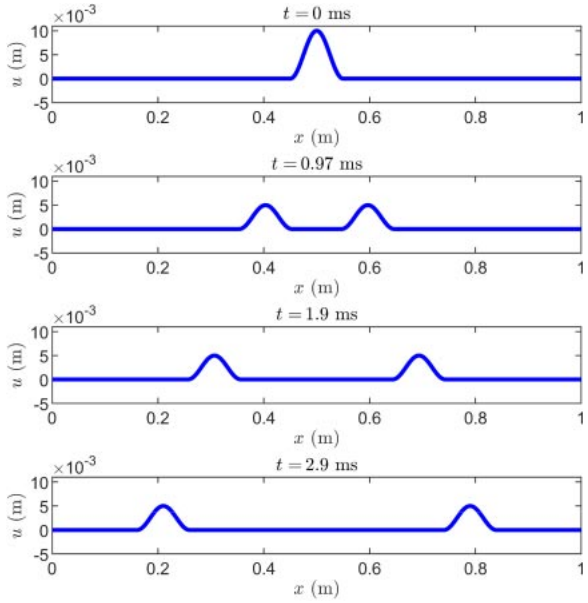

Fig. 2 Time evolution of the solution to the wave equation, at times as indicated, with $c = 100\,\mathrm{m{\cdot}s^{-1}}$, and with a localised initial displacement condition.

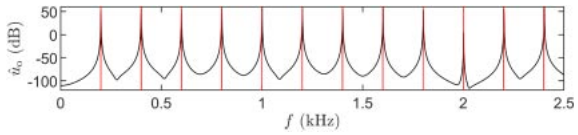

Fig. 3 Spectrum of output drawn from the solution to the one-dimensional wave equation (1). Modal frequencies, multiples of a fundamental frequency of 200 Hz, are shown as red lines for reference.

$$f_p = \frac{cp}{2L} \quad p = 1, \ldots \tag{9}$$

The lowest of these frequencies, $f_1 = c/2L$, is referred to as the fundamental frequency, and corresponds roughly to the pitch of the sound produced. See Fig. 3, showing a Fourier transformed output spectrum drawn from the solution to the wave equation, and illustrating the equally-spaced set of harmonics from (9) above.

2.2. Stiff String Vibration

The wave equation (1) describes the vibration of a perfectly flexible (or very thin) string. As the string thickness increases, effects of stiffness become non-negligible. Stiffness effects in a tensioned string are well described by the following equation:

$$\rho A \partial_t^2 u - T \partial_x^2 u + EI \partial_x^4 u = 0. \tag{10}$$

Here, E is Young's modulus for the string material, in Pa, and I is the moment of inertia in m^4 (and equal to $\pi r^4/4$ for a string of radius r). In the absence of tension, (10) reduces to the Euler-Bernoulli model of transverse beam vibration; similarly, for very thin strings, the one-dimensional wave

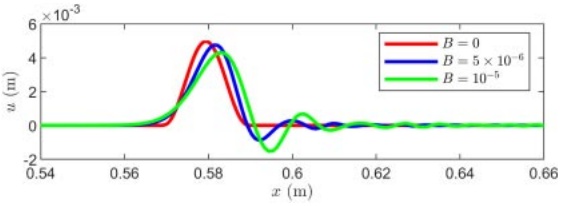

Fig. 4 Dispersion of a rightward traveling pulse on a string, under non-stiff conditions (red), and for increasing stiffness, characterised by the inharmonicity parameter B (blue and green).

equation (1) is recovered. More refined models of the stiff string have been studied in the context of musical acoustics, including the Timoshenko model [24], employed in models of piano strings [25]. For musical strings of typical thicknesses, however, recent studies [26] suggest that such refined models lead to negligible improvement relative to the Euler-Bernoulli model at audible frequencies.

2.2.1. Dispersion and inharmonicity

Employing the same analysis of a wave-like solution as in Sect. 2.1.1, a distinct expression for phase velocity results:

$$\omega = \pm ck\sqrt{1 + \frac{EI}{T}k^2} \quad \rightarrow \quad v_\phi = \pm c\sqrt{1 + \frac{EI}{T}k^2} \geq c. \tag{11}$$

Wave propagation is thus dispersive in a stiff string, with high frequency components traveling progressively faster than low frequency components. This effect is most pronounced in thick strings (as in the case of piano notes in the low register [27]). See Fig. 4, showing a comparison between the propagation of a pulse in a string, for different degrees of stiffness (characterised by the parameter B, as defined in (13) below). Short wavelength (high frequency) components of the solution lead the main pulse. The traveling wave solution (6) is no longer valid in the case of the stiff string (or indeed any modification to the one-dimensional wave equation (1)).

Equation (10) is now of fourth order (in space), and thus requires two boundary conditions at each end of the domain. There are many choices—for strings, it is natural to retain the fixed end conditions (7). A good choice of analytically tractable additional conditions is of those of simply supported type:

$$\partial_x^2 u|_{x=0,t} = \partial_x^2 u|_{x=L,t} = 0 \quad \forall t \geq 0. \tag{12}$$

In this case, the string is able to pivot about its endpoints. Other conditions (such as, e.g., clamped [28]) are possible as well, but given that the effects of stiffness are small relative to that of tension in a string, the choice of simply supported conditions over clamped conditions does not

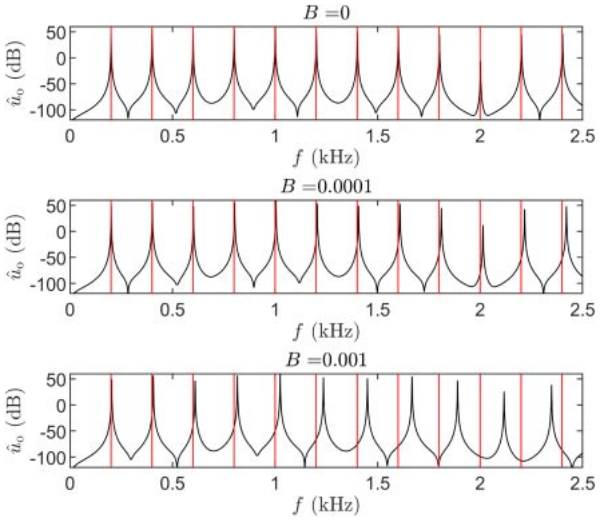

Fig. 5 String spectra, for different values of inhamonicity B, as indicated. The top panel, with $B = 0$, corresponds to the dispersionless case of the wave equation (1). Nominal modal frequencies, for the wave equation without stiffness, and at multiples of a fundamental frequency of 200 Hz, are shown as red lines for reference.

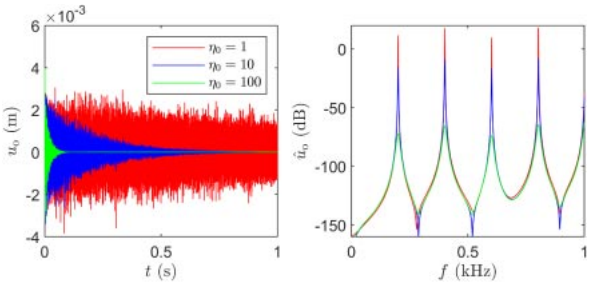

Fig. 6 Output waveforms (left) and magnitude spectra (right) for output drawn from string displacement, under different choices of the loss parameter η_0, as indicated. Here, the string has a fundamental frequency of 200 Hz, and $B = 0.0001$.

lead to major differences in the behaviour of the model. See [29] for a comparison of the two boundary condition choices.

Under these conditions, the modal form of the solution given in (8) in the case of the wave equation holds, but the natural frequencies are modified as [29]:

$$f_p = \frac{cp}{2L}\sqrt{1 + Bp^2} \quad B = \frac{EI\pi^2}{TL^2}. \tag{13}$$

Here, the consolidated parameter B is referred to as the inharmonicity (though slight variations of this expression are sometimes employed [30]). The main effect is a progressive "stretching" of the frequencies of partials above baseline values at multiples of $f_1 = c/2L$. See Fig. 5.

2.3. Loss

The stiff string model presented above is lossless—real string vibration depends crucially on multiple loss mechanisms, leading to a characteristic frequency- or mode-dependent decay time [31].

As a starting point, consider the simplest extension of the stiff string equation (10) to include a dissipation mechanism:

$$\rho A \partial_t^2 u - T\partial_x^2 u + EI\partial_x^4 u + 2\rho A\eta_0 \partial_t u = 0 \tag{14}$$

in terms of the new parameter $\eta_0 \geq 0$.

To analyse solutions to this equation, again consider an infinite domain $x \in \mathbb{R}$, and examine damped wave-like solutions of the form

$$u(x,t) = \hat{u}e^{st - jkx} \tag{15}$$

for complex frequencies $s = j\omega + \sigma$, where σ represents loss. Inserting (15) into (14) leads to the following characteristic equation relating complex frequency s and wavenumber k:

$$s^2 + c^2k^2 + (EI/\rho A)k^4 + 2s\eta_0 = 0 \tag{16}$$

Separating this equation into real and imaginary parts gives:

$$\omega \approxeq \pm ck\sqrt{1 + \frac{EI}{T}k^2} \quad \sigma = -\eta_0 \tag{17}$$

The rate of loss σ is thus constant at all frequencies. In addition, under low loss conditions (typical in strings), the dispersion relation is only altered slightly, and thus mode frequencies are little affected by the addition of loss. See Fig. 6, illustrating the characteristic decay of waveforms, and broadening of resonance peaks in the magnitude spectrum due to loss.

Realistic loss models for strings are far more complex—see Cuesta and Vallette for details [31]. The main contributing mechanisms are air viscosity and internal friction (which itself includes various effects such as viscoelasticity of the string material, heat transport and material dislocations). The model is often framed in terms of a frequency-dependent quality factor $Q(\omega)$, that may be related to the damping factor $\sigma = \sigma(\omega)$ by $Q = -\omega/\sigma$. The frequency dependence of Q depends in a non-trivial way on material parameters, string radius and tension; for musical strings, there is often a pronounced peak in the low kHz range. See Fig. 7.

In the setting of time domain simulation, simplified forms approximating frequency-dependent loss have been employed by various authors. One choice is [32]:

$$\rho A \partial_t^2 u - T\partial_x^2 u + EI\partial_x^4 u + 2\rho A\eta_0 \partial_t u - 2\rho A\eta_1 \partial_t \partial_x^2 u = 0 \tag{18}$$

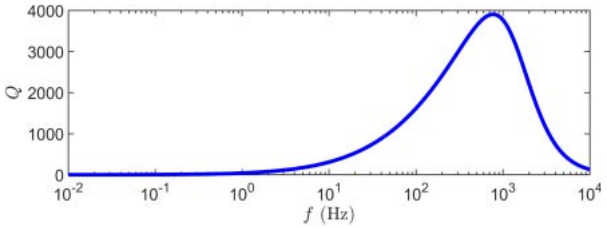

Fig. 7 Quality factor Q, as a function of frequency f in Hz, for a steel string of radius 0.2 mm, and under a tension of 20 N.

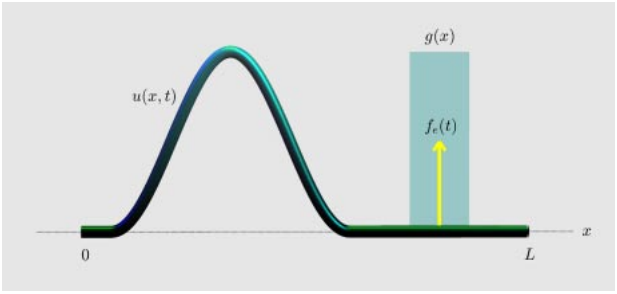

Fig. 8 String subject to an external force f_e over a spatial distribution $g(x)$.

which gives two parameter (η_0 and η_1) control over the quality factor Q. Slightly different models, employing a third time derivative, have been employed by other authors [9,15].

3. EXCITATION AND COLLISION

Though initialisation of the string can be employed as an analysis tool, in practice, a string should more properly be assumed to be at rest initially, and subjected to an external forcing, usually sharply localised at a particular location on the string (i.e., the plucking or striking or bowing position). Assuming a linear model of string vibration, a generalisation of the linear string to include forcing may be written as

$$\mathcal{L}u = g(x)f_{\mathrm{e}}(t). \tag{19}$$

Here, $\mathcal{L}$ represents the ensemble of linear operators appearing in any of the string models presented so far, such as (1), (10), (14) or (18). The distribution $g(x)$ characterises the spatial extent of the excitation, and is normally sharply localised. It is also helpful to assume that it is of unit area, so that

$$\int_0^L g(x)dx = 1. \tag{20}$$

For practical purposes, and also in simulation, it is useful to make use of the idealised case of forcing at a single point, through the use of $g(x) = \delta(x - x_{\mathrm{e}})$, where $\delta(x - x_{\mathrm{e}})$ is a Dirac delta function selecting the excitation location $x = x_{\mathrm{e}}$. Under the normalisation condition (20), f_{e} has units of N, and is the force applied, in the upward direction over the distribution $g(x)$. f_{e} will normally not be independent of the string state u, and in general, Eq. (19) is nonlinear. Depending on the model, f_{e} may result from coupling of the string with a system with its own internal dynamics, as in the case of the hammer-string interaction. See Fig. 8.

Equation (19), beyond modeling an excitation, also models passive (unforced) interactions due to pointwise collisions of the string with an obstacle (such as a fret), and thus a unified presentation follows here. In the case where such collisions occur over a distributed region (as in, e.g., over a fretboard, or in instruments such as the tanpura [33]), a generalisation of (19) is necessary. See Sect. 3.4.

3.1. The Hammer-String Interaction

The hammer-string interaction can be modelled, in the simplest case, as the collision of a mass M kg with a string at a given location x_{e} along its length (characterised by a function $g(x)$ peaked around $x = x_{\mathrm{e}}$), and exerting an upwards force f_e N over the course of the interaction. In this case, the vertical position of the hammer tip is $u_{\mathrm{h}}(t)$, and its dynamics are described by Newton's second law, under the action of the equal and opposite force $-f_{\mathrm{e}}$:

$$M\frac{d^2u_{\mathrm{h}}}{dt^2} = -f_{\mathrm{e}}. \tag{21}$$

f_{e} must always be positive, and one common model [15] is in terms of the interpenetration of the string into the hammer felt, with a power law compression characteristic [34]:

$$f_{\mathrm{e}} = K[u_{\mathrm{h}} - u_{\mathrm{s}}]_+^{\alpha} \quad u_{\mathrm{s}}(t) = \int_0^L g(x)u(x,t)dx. \tag{22}$$

Here, K is a stiffness constant, and $\alpha \geq 1$ is a nonlinearity exponent, to be determined by experiment. $u_{\mathrm{h}} - u_{\mathrm{s}}$ is a measure of distance between the hammer tip and the string at the striking location, with the finite excitation width $g(x)$ taken into account—many authors use a pointwise excitation, so that $g(x)$ is effectively a Dirac delta function [30,35]. The operation $[\eta]_+ = (1/2)(\eta + |\eta|)$ restricts the force to be non-zero only when there is contact between the string and hammer. See Fig. 9 at left. More complete models of the hammer-string interaction take into account damping processes [36] in, e.g., the hammer felt.

In simple models [15], for a single strike, the hammer is assumed to have an initial displacement $u_{\mathrm{h}}(0) = u_{\mathrm{h},0}$ and upward velocity $du_{\mathrm{h}}/dt|_{t=0} = v_{\mathrm{h},0}$. Shown at right in

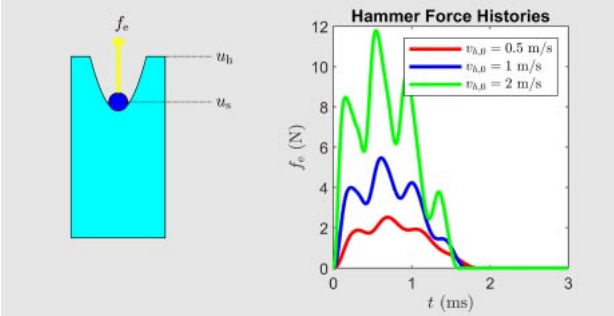

Fig. 9 Left: hammer configuration, side view, with hammer tip position u_h, and the string position u_s indicated in blue. Right: force histories f_e as a function of time, for a steel piano string tuned to C4, and under hammer and string parameters as given in [16]. Force histories are shown for different initial hammer velocities $v_{h,0}$, as indicated.

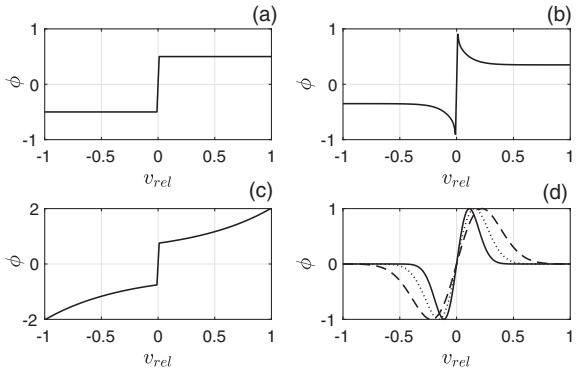

Fig. 10 Bow friction coefficient functions, as a function of relative velocity. (a): Coulomb dry friction; (b): "classical" friction curve (from [42]); (c): "reconstructed" friction curve (from [43]); (d): soft friction curves (from [28]).

Fig. 9 are force histories $f_e(t)$ for strikes at different velocities $v_{h,0}$, as indicated, and with $u_{h,0} = 0$. Notice the appearance of humps in the force histories, due to multiple reflections of waves from the string endpoints back to the hammer while the hammer is in contact with the string. Perceptually, the main effect of increased strike velocity is increased brightness, due to the nonlinearity of the hammer-string contact.

The plucking mechanism (in, e.g., the guitar or harp) is significantly more complex—see, e.g. [37]. It has also been modeled using (19), where the dynamics of the nonlinear plucking mechanism are bypassed through the use of a short externally-supplied function $f_e(t)$ [38].

3.2. The Bowing Mechanism

As mentioned in the introduction, bowed string vibration is a topic of longstanding interest in musical acoustics. Early experimental observations were carried out by Helmholtz using a self-made experimental machine that he called the "vibration microscope" [5]. He observed that motion undergoes a sticking phase, where the string is dragged by the bow, followed by a slipping phase, where the string slides across the bow, once per period. These phases repeat cyclically and give rise to a type of motion often referred to as "Helmholtz motion" [39], or "stick-slip" motion.

These observations were consolidated into a mathematical theory by Raman [6]. He considered an undamped string with no stiffness, excited by a force dependent on the relative velocity between the bow and the string at one point. With these assumptions, Raman obtained an analytically tractable system of equations. Schelleng extended the results by Raman to produce "Schelleng diagrams" [39]: these are regions of the bow force - bow position plane in which musical tones are produced. Guettler diagrams are similar, but consider bow acceleration instead of bow position [40].

Raman's work paved the way for many successive works, by framing the string-bow interaction in terms of a friction force depending on the relative velocity between string and bow. In this framework, the equation of the bowed string may be cast in the form of (19) with

$$f_e = -F_B \phi(v_{\rm rel}). \tag{23}$$

Just as in the case of the hammer-string interaction, $g(x)$ may be assumed to be a Dirac distribution $\delta(x - x_B)$, where x_B is the bow position, though finite-width effects have been shown to play a role in determining the torsional motion of the string [41]. In Eq. (23), the function ϕ describes the friction force normalised by the normal load, and is referred to as *friction curve* (it is, in fact, a dimensionless friction coefficient). The relative velocity is defined as

$$v_{\rm rel} = \int_0^L g(x) \partial_t u \, {\rm d}x - v_B, \tag{24}$$

where v_B is the velocity of the bow, assumed known. Finally, F_B is the normal bow force, also assumed known.

Various friction characteristic curves have been studied, and examples are shown in Fig. 10. A classic dry friction model, as per the Coulomb theory, is shown in Fig. 10(a): here, the absolute value of the force is independent of the relative velocity. A more refined approximation is due to Smith and Woodhouse, who performed experimental studies of the motion of a mass on a rosin-coated conveyor belt [42]; see Fig. 10(b) [42]. Here, during the first instants of slipping the magnitude of the friction force decreases as the relative velocity becomes larger, until it attains a steady value. This curve is sometimes called the "classical" friction curve in the

context of the bow-string interaction [43]. Curves analogous to this had in fact been employed in earlier works, such as those by Friedlander [7] and by McIntyre and Woodhouse [18]. Galluzzo proposed the curve in Fig. 10(c), after measuring the force drop at the bridge during the slip phase: this curve has been called the "reconstructed" friction curve [43]. In the context of numerical simulation, a family of friction curves as shown in Fig. 10(d) has been proposed, where a free parameter allows control over the steepness of the central slope [28].

The friction curve models constitute a useful framework for understanding the bowing mechanism. Indeed, when these models are used for simulation, it is possible to reproduce most of the main features observed in practice: these include Helmholtz motion, raucous motion, multi stick-slip motion, anomalous low-frequency waves, and others [44]. See also Fig. 11. However, detailed experimental evidence suggests that these models are in fact too simple for an accurate representation of the bow-string interaction. Note that in (23), it is assumed that the friction coefficient ϕ depends exclusively on the relative velocity. The friction properties of rosin, however, show some dependence on temperature, and for this reason Smith and Woodhouse have proposed a model incorporating thermal exchanges [42]. This model is able to reproduce the hysteretic behaviour of the friction curve observed experimentally, but nonetheless discrepancies with respect to experiment remain [43].

In order to account for the hysteretic behaviour of the friction curve, a different class of models has also been proposed, incorporating the effects of the bristle-string interaction. These include the Dahl model, the LuGre model, and an elasto-plastic model; see Serafin for a review [45].

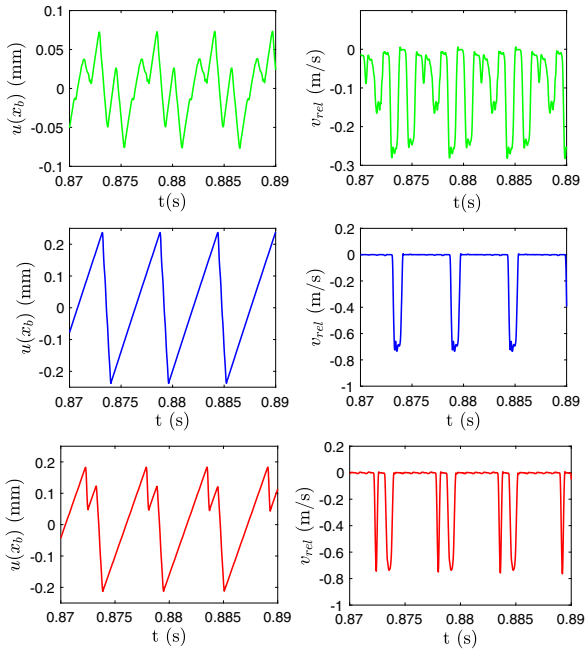

Fig. 11 Simulated displacement at the bowing point and relative velocity for a bowed string at different bowing forces. At a low force (green), the string does not stick to the bow, and raucous motion is observed. For higher bowing forces (blue), the string presents the typical "stick-slip" behaviour associated with Helmholtz motion. At even higher bowing forces (red), multiple stick-slip phases are observed.

3.3. Collision with a Point Obstacle

Various timbres generated by stringed instruments rely on a collision mechanism. In some cases, such as the hammer-string interaction discussed in Sect. 3.1, the colliding object is moving. In many other cases, such as the string-fretboard interaction in the guitar, the string collides against immovable point obstacles.

As a useful starting point, here a single lumped obstacle occupying a small region around $x_c \in \mathcal{D}$ is considered. The mathematical model given in (19) applies again in this case. Here, the spatial distribution of the obstacle is described by the function $g(x)$, which satisfies the normalisation property (20). Again, in practice, such a distribution may take the form of a Dirac delta function $\delta(x - x_c)$, or any other strongly localised function centered around x_c. Let b denote the obstacle's height measured from the string rest position, with the obstacle placed below the string. An expression for the force experienced by the string is

$$f_e = K[b - u_s]_+^\alpha \quad u_s(t) = \int_0^L g(x)u(x,t)dx. \qquad (25)$$

This form resembles (22), but the physical interpretation is different. In the hammer-string interaction, the power law (22) can be viewed as permitting some level of deformation of the hammer felt. In the string-obstacle interaction, both objects are undeformable, and the interpenetration $[b - u_s]_+$ is spurious. In the context of numerical simulation, model (25) has nonetheless proven useful in treating the string-obstacle interaction. Issanchou *et al.* [46] showed that this model yields a very close match to the analytic results given by Cabannes [47], for a string colliding against a fret placed halfway along the string. Indeed, one can make the the spurious interpenetration as small as desired by increasing the value of the stiffness constant K—see Bilbao *et al.* [48]. In Fig. 12, snapshots of a string colliding against a rigid obstacle are shown. In Fig. 13, the time history of the string displacement at the obstacle location x_c is given, under various choices of the stiffness constant K. Note that the resulting dynamics are strongly nonlinear, including a strong biasing effect on the string displacement during collision.

Extensions of model (25) to the case of multiple point obstacles is immediate: the total force experienced by the

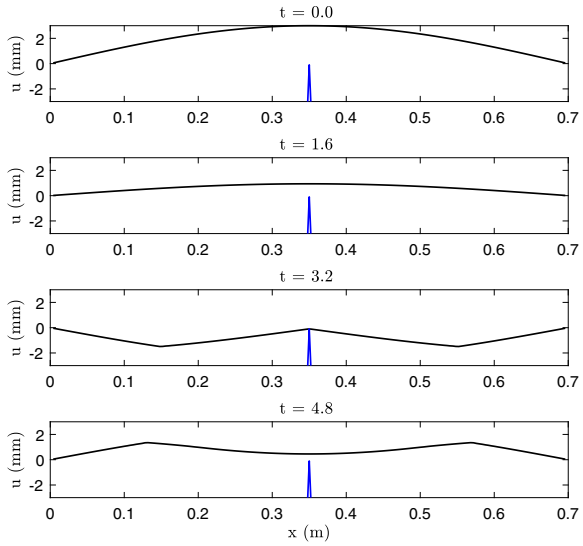

Fig. 12 Snapshots of string-fret collision, at times indicated (in ms). Here, the string is described by the simple wave equation (1), with $c = 175.9\,\mathrm{m/s}$. The fret is located at the centre of the string, of length $L = 0.7\,\mathrm{m}$. The barrier coefficients are stiffness $K = 10^{17}$, exponent $\alpha = 1.1$, and $b = -1\,\mathrm{mm}$. The string is initialised in its first mode of vibration, given by $u_0(x) = U_0 \sin(\pi x/L)$, with $U_0 = 3\,\mathrm{mm}$.

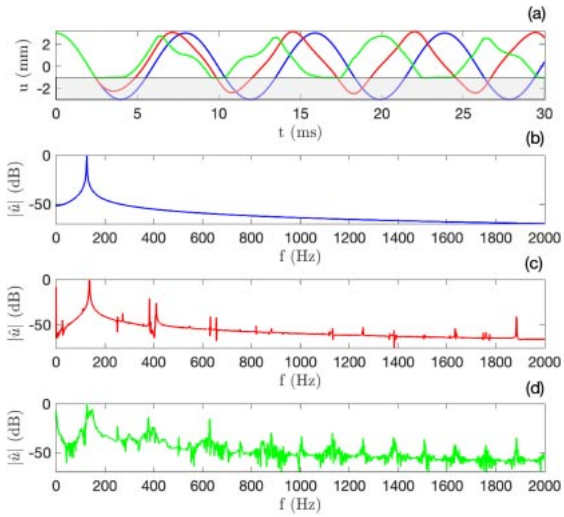

Fig. 13 String-fret collision, role of the barrier stiffness constant. Here, the string and the barrier are as per Fig. 12, except for the barrier stiffness constant, which is chosen here as $K \in \{0, 10^3, 10^{17}\}$. (a): time domain solutions, recorded at the barrier location. In this plot, the blue line corresponds to the case $K = 0$; the red line to $K = 10^3$; the green line to $K = 10^{17}$; the shaded area represents the barrier. The role of the nonlinear collision is clearly represented in the spectra. (b): $K = 0$ (no barrier) the string vibrates in its first mode. (c): $K = 10^3$ (soft barrier), other modes are activated by the collision (note that here the string is able to interpenetrate the barrier by a finite amount). (d): $K = 10^{17}$ (hard collision), the collisions produce strong wideband modal couplings.

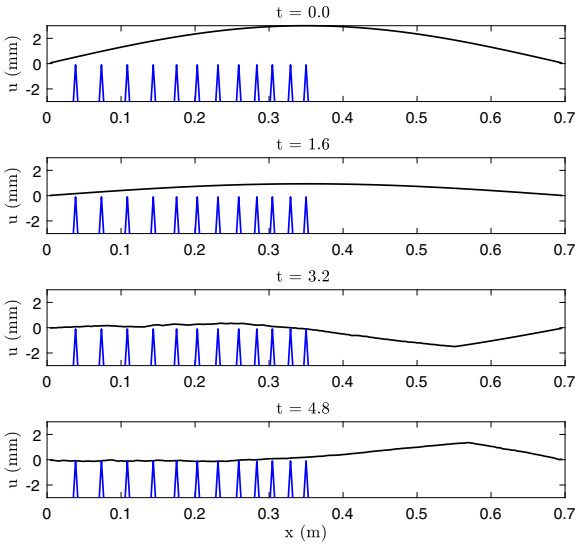

Fig. 14 Snapshots of string-bridge collision, at times indicated (in ms) in the presence of frets separated by a semitone. Here, the ith fret is located at $x_{b_i} = L(1 - 2^{-\frac{i}{12}})$, and $i = 1, \ldots, 12$. The string and obstacle parameters are the same as Fig. 12.

string is just the sum of the contributions coming from a each of the obstacles. See Fig. 14.

Model (25) has served as the basis for many works simulating the string-obstacle interaction, see e.g. [46,48–50], but various other methods exist in the literature. Evangelista and Eckerholm proposed a digital waveguide method incorporating collision scattering junctions [51] (see also Sect. 5.1 for a review on digital waveguides). Debut and Antunes made use of the Udwadia-Kalaba formalism to frame the finger-string interaction in terms of a constrained modal system [52].

3.4. Distributed Collisions

In many musical stringed instruments, the string collides against objects with a finite spatial extent. In traditional Indian instruments, such as the sitar and the tanpura, the string wraps against a bent bridge, resulting in a characteristic droning sound.

Many works have studied the effects of collisions of the string against distributed objects. Burridge *et al.* [53], inspired by the works of Raman [6], gave analytic results for the case of a thin string wrapping against a bent bridge, when the string is initialised in the first mode of vibration and the collisions are inelastic. Successive works have considered the problem of the string-bridge interaction: Alsahlani and Mukherjee presented a semi-analytic model for bridges of circular and elliptical cross sections [54]; Mandal and Wahi gave analytic results for the natural frequencies and mode shapes of the string in the presence of the bridge [55].

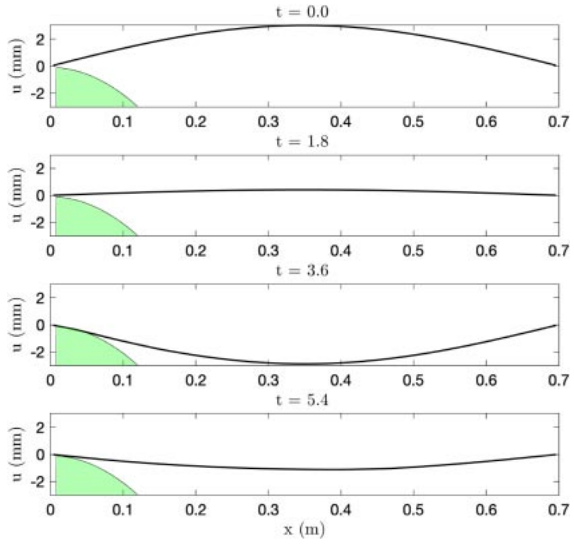

Fig. 15 Snapshots of string-bridge collision, at times indicated (in ms) in the presence of a curved bridge. The string parameters are the same as Fig. 12. The barrier is given here by $b(x) = -10^{-4} - 2 \cdot 10^{-1}x^2$.

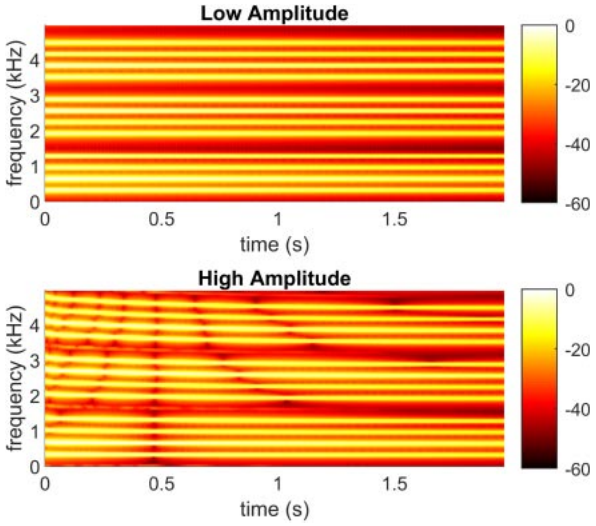

Fig. 16 Spectrograms of output grawn from the Kirchhoff-Carrier model, under low amplitude excitation (top) and high amplitude excitation (bottom), illustrating the characteristic pitch glide in the latter case. In this case, the string is made of steel, and is of radius $r = 0.1$ mm, and is under a tension of $T = 100$ N.

Mathematically, the problem of distributed collisions can be framed in a very similar fashion as (19), that is

$$\mathcal{L}u = F_{\mathrm{e}}(x,t), \tag{26}$$

where

$$F_{\mathrm{e}}(x,t) = K[b(x) - u(x,t)]_+^{\alpha}. \tag{27}$$

Here, height of the distributed barrier is described by the function $b(x)$. The right-hand side of (26) represents a force density, in N/m, distributed along x. This model served as the basis for numerous works dealing with the numerical simulation of distributed collisions is strings: these include Chatziioannou and van Walstijn [33]; Bilbao *et al.* [48]; Issanchou *et al.* [46]; Ducceschi *et al.* [50]. See also Fig. 15.

4. NONLINEAR STRING VIBRATION

All of the models presented in Sect. 3 include a nonlinearity, either in the definition of the excitation mechanism, or through a unilateral constraint. The underlying string model, however, remains linear. Under high amplitude vibration, the behaviour of a vibrating string departs from linear, even in the case of free vibration. In this section, two such geometrically nonlinear models are presented—both generalise the one-dimensional wave equation (1), and, for simplicity, effects of linear stiffness are not included here (though they can be reintroduced in a subsequent step).

The theory of the nonlinear elastic vibration of a string was the subject of extensive research for more than a century, dating back as far as the work of Kirchhoff [56]. Major contributions were due to Carrier [57], Oplinger [58], Anand [59], Narasimha [60] and O'Reilly and Holmes [61]. See the texts of Morse and Ingard [62] and the chapter by Vallette [63] for an overview.

4.1. Kirchhoff-Carrier Model

The simplest nonlinear model of string vibration is often ascribed to Kirchhoff [56] and Carrier [57]:

$$\rho A \partial_t^2 u - T\left(1 + \frac{EA}{2TL}\int_0^L (\partial_x u)^2 dx\right)\partial_x^2 u + 2\rho A \eta_0 \partial_t u = 0. \tag{28}$$

The main difference, with respect to the linear wave equation (1) is the multiplication of the tension by a scalar amplitude-dependent factor, always greater than 1. Grossly-speaking, this factor leads to an increase in the wave speed with solution amplitude. An additional loss term has been included, in line with (14), so as to illustrate the effect of so-called pitch glides (see below). The Kirchhoff-Carrier model has seen extensive theoretical investigation outside of musical acoustics [58,64,65], and later, in the context of musical strings [66,67]. The Kirchhoff-Carrier model was the first geometrically nonlinear string model to be used for synthesis purposes [68–72], partly due to the simple scalar form of the nonlinearity.

The most important perceptual effect of the Kirchhoff-Carrier nonlinearity is the pitch glide, audible under struck or plucked conditions at high amplitudes. See Fig. 16. Here, towards the start of a note, the effective wave speed is increased, and gradually decreases to the nominal (linear) wave speed as dissipation effects reduce vibration

amplitude. As such, the particular loss model employed, including its frequency dependence, as discussed in Sect. 2.3, is strongly related to the pitch trajectory of the glide itself.

4.2. Full Geometrically Nonlinear Model

The Kirchhoff-Carrier is a crude first approximation to the nonlinear dynamics of a string. Moving to a full model of nonlinear string vibration necessarily requires introducing coupling between transverse displacement, written here as $u(x,t)$, and longitudinal displacement, written here as $w(x,t)$. A general model is of the form of a pair of coupled partial differential equations [62]:

$$\rho A \partial_t^2 u - EA\partial_x^2 u + \partial_x \left(\frac{(EA - T)\partial_x u}{\sqrt{(\partial_x u)^2 + (1 + \partial_x w)^2}} \right) = 0 \quad (29a)$$

$$\rho A \partial_t^2 w - EA\partial_x^2 w + \partial_x \left(\frac{(EA - T)(1 + \partial_x w)}{\sqrt{(\partial_x u)^2 + (1 + \partial_x w)^2}} \right) = 0 \quad (29b)$$

The model now exhibits amplitude-dependent effects. See Fig. 17, illustrating the time evolution of an initial transverse displacement condition at different amplitudes.

At low displacements, the two equations uncouple into two distinct one-dimensional wave equations:

$$\rho A \partial_t^2 u - T\partial_x^2 u = 0 \quad \rho A \partial_t^2 w - EA\partial_x^2 w = 0. \quad (30)$$

The first is simply the one-dimensional wave equation in transverse displacement (1), with wave speed $c = \sqrt{T/\rho A}$. The second is a one-dimensional wave equation with wave speed $c^{(l)} = \sqrt{E/\rho}$. This equation governs longitudinal wave propagation. In general, $c^{(l)} \geq c$ for musical strings. As a result, under fixed boundary conditions for both u and w, and under low amplitude conditions, two sets of modal frequencies are present:

$$f_p = \frac{cp}{2L} \quad f_p^{(l)} = \frac{c^{(l)} p}{2L} \quad p = 1, \ldots \quad (31)$$

When the equations are coupled, as in (29), wave propagation undergoes distortion with respect to the linear model—see Fig. 18. A primary perceptual effect is the introduction of new frequency components, at sum and difference frequencies between the two modal frequency series given in (31). See Fig. 19, illustrating the spectra of struck strings under increasing strike amplitudes. It has been proposed [73] that the nonlinear coupling between longitudinal and transverse motion of the string is the origin of so-called phantom partials in piano tones. Though the model (29) does indeed produce additional inharmonic partials due to nonlinear mixing, it has been suggested recently that this effect may not be the major contributor to observed phantom partials in the piano, which may be due to interaction between the strings and structural components [74].

The model (29) has been employed, including linear stiffness and losses, and using series-approximated forms of the nonlinearity, for sound synthesis purposes [75,76], and the full model has been used in a complete model of

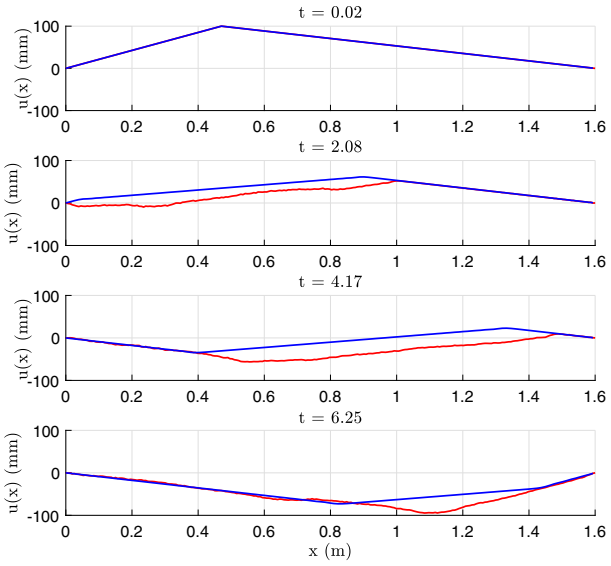

Fig. 17 Snapshots of the time evolution of solutions to the linear (blue line) and nonlinear (red line) wave equations, at times indicated (in ms). Here, the string is initialised with a triangular distribution with large peak amplitude (100 mm). The key features of nonlinear wave propagation relative to linear are increased wave speed, as well as a progressive flattening of the wavefront with time.

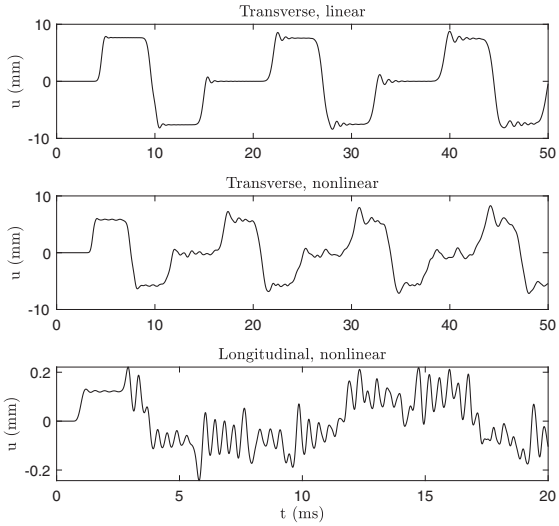

Fig. 18 Linear, transverse nonlinear and longitudinal nonlinear output waveforms, for a steel string of length $L = 1$ m, radius $r = 0.3$ mm, tension $T = 30$ N. The string is struck with a hammer-like force. Note the pulse distortion of the wavefront in the nonlinear transverse case compared to linear, as well as the high-frequency vibration of the longitudinal waves.

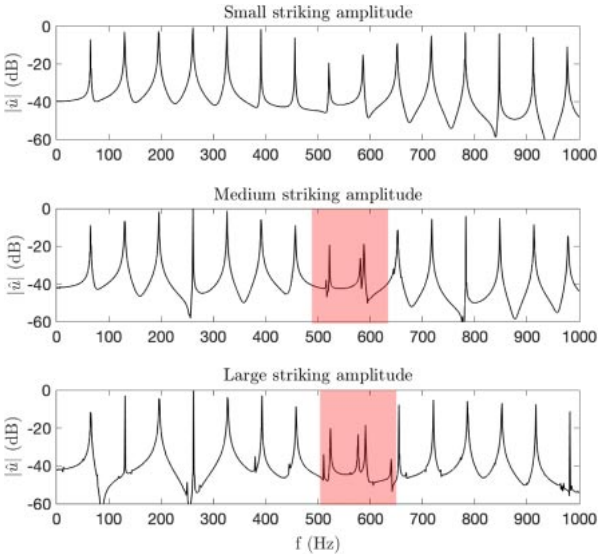

Fig. 19 Output transverse spectra of the geometrically exact nonlinear string, for a string with fundamental frequency of 63 Hz, and physical parameters typical of piano strings. At low amplitude, the peaks correspond to the linear natural frequencies of the string. As the strike force increases, "phantom partials" appear as a consequence of the nonlinear coupling between transverse and longitudinal waves (visible in the shaded areas).

the piano [77], and more recently as the basis for fast numerical simulation techniques [78].

5. NUMERICAL SIMULATION TECHNIQUES

This article is concerned with models of string vibration. In all but the most trivial cases, analytic solutions are not available, and thus numerical approximation is an essential tool, whether the goal is the validation of experimental results, or to generate synthetic sound. The number of numerical techniques that have been applied to different string models is large, and a full theoretical development is not possible here. The basics of some well-known approaches are presented below.

5.1. Digital Waveguides

In the context of sound synthesis, perhaps the best known numerical approximation technique is the digital waveguide method, due to Smith [23,79]. The digital waveguide is extremely efficient as a simulator of linear strings, and is essentially a discrete emulation of the traveling wave solution to the one-dimensional wave equation, as given in (6). Digital waveguides can be viewed as a powerful physical interpretation of the earlier efficient (but non-physical) Karplus-Strong string synthesis method [80], and drew on earlier results on excitation/resonator representations of musical instruments [81].

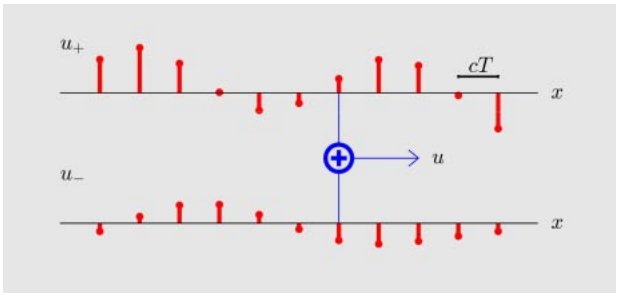

Fig. 20 Graphical representation of the digital waveguide: the physical solution u is a sum of traveling wave components u_+ and u_-, here represented over a spatial grid.

As mentioned above, the starting point for waveguide methods is the traveling wave solution to the one-dimensional wave equation (6). At any location x, the solution may be represented in terms of values drawn from the two distributions $u_+(x)$ and $u_-(x)$, assumed known. Assume now a sample rate F_s, and an associated time step $T = 1/F_s$. Suppose now that these initial distributions are sampled, spatially to yield the sequences $u_+[l]$ and $u_-[l]$, as:

$$u_+[l] = u_+(x = lcT) \quad u_-[l] = u_-(x = lcT) \tag{32}$$

The discrete time solution $u^n[l]$ may thus be written as

$$u^n[l] = u_+[l - n] + u_-[l + n] \tag{33}$$

This representation is exact in the case of the one-dimensional wave equation, and has the interpretation of a pair of digital delay lines, requiring only shifts of data and minimal arithmetic—the key to the performance advantage of digital waveguides. When the string is of finite length, a termination condition is required at either end of the domain (usually reflection with inversion), feeding values from u_+ to u_- and vice versa. See Fig. 20.

More realistic string modeling requires the introduction of the effects of stiffness and loss, as in Sects. 2.2 and 2.3. In this case, the traveling wave solution no longer holds, but it is possible to "lump" such effects using carefully-designed terminating filters at the string ends. See, e.g., [82,83]. Digital waveguides have been employed for synthesis for a variety of stringed instruments beyond bowed strings [84] (their first use [79]), including the guitar [51,85,86], harpsichord [87], piano [32,88], the Clavinet [89] and the Finnish kantele [71] among many others.

5.2. Modal Methods

Modal simulation techniques for physical modeling synthesis developed at roughly the same time as digital waveguide methods. Time-invariance and linearity allow the description of a spatially-distributed system, such as a

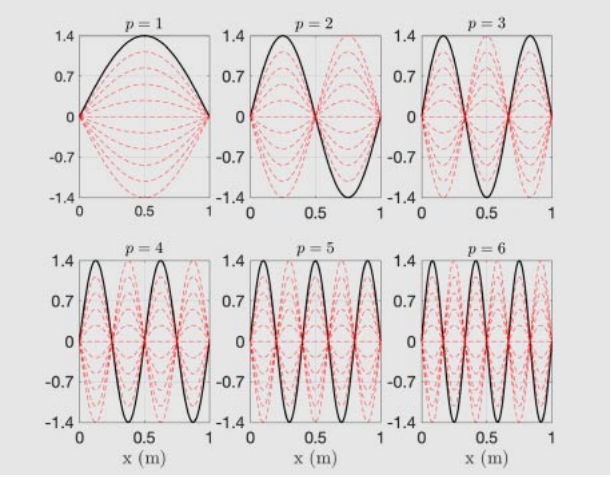

Fig. 21 First six modes for a fixed-fixed string.

string, in terms of eigenfunctions and frequencies, called the *modes* of the system. Such modal shapes and frequencies may be either determined experimentally, or starting from a suitable mathematical model. The solution $u(x,t)$ of a given model problem, defined over a finite domain such as $x \in [0, L]$, such as one of the linear string models described in Sect. 2, is written as the sum of "modes", i.e.

$$u(x,t) = \sum_{p=1}^{\infty} \phi_p(x) q_p(t). \tag{34}$$

Here, $\phi_p(x)$, $p = 1, \ldots,$ is the series of modal shapes, normally an orthonormal set over the problem domain. $q_p(t)$ is the corresponding time-dependent amplitude. For example, modal shapes resulting from fixed boundary conditions in the case of the linear non-stiff string were described in Sect. 2.1.2 are are illustrated in Fig. 21. Under unforced conditions, the amplitudes $q_p(t)$ have the form of pure sinusoids, as in (8).

Modal simulation methods result from the projection of (34) onto the modal shapes ϕ_p, and the truncation to a finite number (say M) of modes, in preparation for discrete time simulation. Orthogonality of the modal shapes leads to an uncoupled system of ordinary differential equations:

$$\ddot{q}_p(t) = -\omega_p^2 q_p(t) - \xi_p q_p(t) + f_p(t) \quad p = 1, \ldots, M. \tag{35}$$

In the above, ω_p and ξ_p are the natural frequencies and the decay constants of the pth mode. Finally, f_p is a driving term, resulting from the projection of a source distribution onto the pth modal shape. The uncoupled second order equations above are easily transferred to discrete time through various numerical integration techniques.

This approach lends itself naturally to the efficient simulation of mechanical vibrations, and thus to sound synthesis via physics-based modelling. Modal synthesis began in earnest in the 1990s, when frameworks such as Mosaic [90] emerged. Due to their efficiency, as well as ease of control over natural frequencies and damping, modal methods gained some popularity, and early modal synthesis software such as Modalys [91] is still being developed today.

Modal methods are best suited to treat problems where the modal shapes and frequencies are known analytically—a small (but important) fraction of the typical systems encountered in musical acoustics. Dynamic rendering and control are also problematic, since each input/output requires the storage of the corresponding array of modal weights. Furthermore, extensions of modal methods to nonlinear cases are difficult (see e.g. [46,92]), as is the treatment of system with complex geometries or space-variant parameters.

5.3. Time Domain Methods

Mainstream time-stepping methods, such as the finite difference time domain method (FDTD) [93,94] sacrifice the efficiency advantage of digital waveguides, but at the same time allow for the simulation of much more general string vibration problems, including all of the features described in this article. The key distinction with regard to a method such as modal synthesis, is that all operations occur locally; there is no projection stage. This simplifies the treatment of phenomena best modelled locally, such as excitations, and also boundary conditions. Pioneering work using FDTD was carried out by Ruiz [9], and Hiller and Ruiz [10,11], and major advances were made by Chaigne [14] and Chaigne and Askenfelt [15,16]. Many applications to string vibration appear in [28].

As a simple example, consider the linear model of string vibration with frequency-dependent loss, as in (18). Suppose $u(x,t)$ is approximated over a grid, at spatial locations $x = lX$, where integer l is the grid index, and X is the grid spacing, in m, and at times $t = nT$, where integer n is the time index, and T is the time step, in s. A finite difference scheme approximating (18) can be written in terms of the grid function $u^n[l]$, as:

$$\begin{aligned} u^{n+1}[l] = {} & a_0 u^n[l] + a_1(u^n[l+1] + u^n[l-1]) \\ & + a_2(u^n[l+2] + u^n[l-2]) \\ & + b_0 u^{n-1}[l] + b_1(u^{n-1}[l+1] + u^{n-1}[l-1]). \end{aligned} \tag{36}$$

Here, the constants a_0, a_1, a_2, b_1 and b_2 may be written in terms of the defining parameters for (18), as well as T and X [32]. This is a two-step explicit finite difference scheme, allowing the direct recursive calculation of the grid function from previously computed values. Here, $u^{n+1}[l]$ is computed in terms of neighbouring values of the grid function at time steps n and $n-1$ only. See Fig. 22.

The major differences here with respect to digital waveguides are first: generality—the FDTD scheme does

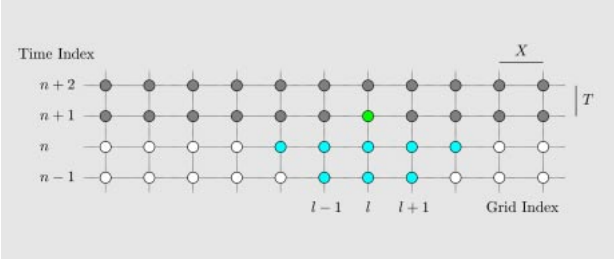

Fig. 22 Graphical representation of the finite difference scheme (36) for system (18), with grid spacing X and time step T. Here, values of the grid function $u^n[l]$ have been computed up through time step n (white circles), and unknown values to be computed are indicated as grey circles. Updating the scheme for the unknown value $u^{n+1}[l]$ (indicated in green) requires values of the grid function at the previous two time steps, and at neighbouring grid locations (indicated in blue).

not rely on particular features of the solution (i.e., a traveling wave decomposition) in order to operate, and second: computational cost, which is significantly higher for the FDTD scheme. In general, an FDTD method will be slightly more computationally costly than a modal approach. Not discussed here is the major issue of ensuring numerical stability for the scheme (36). In this case of a linear system, Fourier techniques such as von Neumann analysis [93] are available and lead, ultimately, to a lower bound on the grid spacing X in terms of the time step T (and, for the one-dimensional wave equation, to the famous Courant-Friedrichs-Lewy condition $X \geq cT$ [95]). For systems involving nonlinearity, however, energy-based techniques are necessary. See, e.g., [25,28,48].

6. CONCLUDING REMARKS

Models of musical vibration of a string can be viewed as a series of successively more refined approximations—much like a set of Russian dolls—with the one-dimensional wave equation (1) at its core. Some of the more exotic variants, such as those including distributed collision and geometric nonlinearities, have only recently begun to see serious scientific investigation, and there remains much to learn. Beyond this, many important features of string vibration have not been covered in this short review article.

In this article, the motion of a string has been restricted to a single plane (perhaps including longitudinal motion, as in Sect. 4.2). However, a full model of string vibration will necessarily include the effects of precession of the plane of vibration, often referred to as "whirling" [61,96,97]. Such fully three-dimensional motion has seen very little research from the point of view of musical acoustics. The torsional, or twisting motion of the string has similarly not been discussed here, but has seen some investigation in the context of bowed string dynamics [98,99].

Furthermore, the string has only been studied in isolation; in all musical instruments, there is necessarily a coupling, through the string terminations, to a bridge mechanism and an instrument body that is ultimately the mechanism responsible for radiating sound. In some numerical studies (of the guitar [38] and piano [25]), a complete model has been successfully built, including acoustic radiation into the 3D space surrounding the instrument. In order to model coupling between the strings and the instrument body, simple boundary conditions such as (7) and (12) must be replaced by conditions allowing the two-way transfer of energy between the string and body. This coupling has been studied for many instrument types. For the piano soundboard, the mechanism for sound radiation, the connection gives rise to subtle phenomena such as the coupling between strings for multiply-strung notes, leading to "two-stage" decay [100]. From a computational standpoint, in the setting of digital waveguides, measured bridge admittances and radiation characteristics are often modeled through a consolidated filter termination [84].

ACKNOWLEDGMENTS

M.D. has received funding from the European Research Council (ERC) under the European Union's Horizon 2020 research and innovation programme, Grant agreement No. 950084 - NEMUS.

REFERENCES

[1] N. Fletcher and T. Rossing, *The Physics of Musical Instruments* (Springer-Verlag, New York, 1991).
[2] D. Campbell and C. Greated, *The Musician's Guide to Acoustics* (Oxford University Press, Oxford, 1994).
[3] A. Chaigne and J. Kergomard, *Acoustique des Instruments de Musique* (Belin, Paris, 2008).
[4] T. Rossing, Ed., *The Science of String Instruments* (Springer-Verlag, New York, 2012).
[5] H. von Helmholtz, *Lehre von den Tonempfindungen* (Druck und Verlag von Friedrich Vieweg und Sohn, Braunschweig, 1862); English edition: *On the Sensation of Tone* (Dover, New York, 1954).
[6] C. Raman, "On the mechanical theory of the vibrations of bowed strings and of musical instruments of the violin family, with experimental verification of the results—Part I," *Bull. Indian Assoc. Cultiv. Sci.*, **15**, 1–158 (1918).
[7] F. Friedlander, "On the oscillations of the bowed string," *Math. Proc. Cambridge Philos. Soc.*, **49**, 516–530 (1953).
[8] J. Keller, "Bowing of violin strings," *Commun. Pure Appl. Math.*, **6**, 483–495 (1953).
[9] P. Ruiz, "A technique for simulating the vibrations of strings with a digital computer," *Master's Thesis, University of Illinois* (1969).
[10] L. Hiller and P. Ruiz, "Synthesizing musical sounds by solving the wave equation for vibrating objects: Part I," *J. Audio Eng. Soc.*, **19**, 462–470 (1971).
[11] L. Hiller and P. Ruiz, "Synthesizing musical sounds by solving the wave equation for vibrating objects: Part II," *J. Audio Eng. Soc.*, **19**, 542–550 (1971).

[12] R. Bacon and J. Bowsher, "A discrete model of a struck string," *Acta Acust. united Ac.*, **41**, 21–27 (1978).

[13] X. Boutillon, "Model for piano hammers: Experimental determination and digital simulation," *J. Acoust. Soc. Am.*, **83**, 746–754 (1988).

[14] A. Chaigne, "On the use of finite differences for musical synthesis. Application to plucked stringed instruments," *J. d'Acoust.*, **5**, 181–211 (1992).

[15] A. Chaigne and A. Askenfelt, "Numerical simulations of struck strings. I. A physical model for a struck string using finite difference methods," *J. Acoust. Soc. Am.*, **95**, 1112–1118 (1994).

[16] A. Chaigne and A. Askenfelt, "Numerical simulations of struck strings. II. Comparisons with measurements and systematic exploration of some hammer-string parameters," *J. Acoust. Soc. Am.*, **95**, 1631–1640 (1994).

[17] J. Schelling, "The bowed string and the player," *J. Acoust. Soc. Am.*, **53**, 26–41 (1973).

[18] M. McIntyre and J. Woodhouse, "On the fundamentals of bowed string dynamics," *Acustica*, **43**, 93–108 (1979).

[19] L. Cremer, *The Physics of the Violin* (MIT Press, Cambridge, Mass., 1984).

[20] J. Woodhouse, "Physical modeling of bowed strings," *Comput. Music J.*, **16**(4), pp. 43–56 (1992).

[21] P. Morse, *Vibration and Sound*, 2nd ed. (Acoustical Society of America, New York, 1981).

[22] J. d'Alembert, "Investigation of the curve formed by a vibrating string, 1747," in *Acoustics: Historical and Philosophical Development*, R. Lindsay, Ed. (Dowden, Hutchinson & Ross, Stroudsburg, 1973), pp. 119–123.

[23] J. O. Smith III, "Physical modelling using digital waveguides," *Comput. Music J.*, **16**(4), pp. 74–91 (1992).

[24] K. Graff, *Wave Motion in Elastic Solids* (Dover, New York, 1975).

[25] J. Chabassier, A. Chaigne and P. Joly, "Time domain simulation of a piano. Part 1: Model description," *ESAIM Math. Model. Num. Anal.*, **48**, 1241–1278 (2014).

[26] M. Ducceschi and S. Bilbao, "Conservative finite difference time domain schemes for the prestressed timoshenko, shear and euler-bernoulli beam equations," *Wave Motion*, **89**, 142–165 (2019).

[27] M. Podlesak and A. Lee, "Dispersion of waves in piano strings," *J. Acoust. Soc. Am.*, **83**, 306–317 (1988).

[28] S. Bilbao, *Numerical Sound Synthesis* (John Wiley & Sons, Chichester, 2009).

[29] H. Fletcher, "Normal vibration frequencies of a stiff piano string," *J. Acoust. Soc. Am.*, **36**, 203–209 (1964).

[30] H. Suzuki, "Model analysis of a hammer-string interaction," *J. Acoust. Soc. Am.*, **82**, 1145–1151 (1987).

[31] C. Cuesta and C. Vallette, "Evolution temporelle de la vibration des cordes de clavecin," *Acustica*, **66**, 37–45 (1988).

[32] J. Bensa, S. Bilbao, R. Kronland-Martinet and J. O. Smith III, "The simulation of piano string vibration: From physical models to finite difference schemes and digital waveguides," *J. Acoust. Soc. Am.*, **114**, 1095–1107 (2003).

[33] V. Chatziioannou and M. van Walstijn, "Energy conserving schemes for the simulation of musical instrument contact dynamics," *J. Sound Vib.*, **339**, 262–279 (2015).

[34] D. Hall and A. Askenfelt, "Piano string excitation V: Spectra for real hammers and strings," *J. Acoust. Soc. Am.*, **83**, 1627–1638 (1988).

[35] D. Hall, "Piano string excitation VI: Nonlinear modeling," *J. Acoust. Soc. Am.*, **92**, 95–105 (1992).

[36] K. Hunt and F. Crossley, "Coefficient of restitution interpretedas damping in vibroimpact," *ASME J. Appl. Mech.*, **19**, 440–445 (1975).

[37] D. Chadefaux, J.-L. LeCarrou, B. Fabre and L. Daudet, "Experimentally based description of harp plucking," *J. Acoust. Soc. Am.*, **131**, 844–855 (2012).

[38] G. Derveaux, A. Chaigne, P. Joly and E. Bécache, "Time-domain simulation of a guitar: Model and method," *J. Acoust. Soc. Am.*, **114**, 3368–3383 (2003).

[39] J. C. Schelleng, "The physics of the bowed string," *Sci. Am.*, **230**, 87–95 (1974).

[40] K. Guettler, "Wave analysis of a string bowed to anomalous low frequencies," *J. Catgut Acoust. Soc.*, **2**(6), pp. 8–14 (1994).

[41] R. Pitteroff and J. Woodhouse, "Mechanics of the contact area between a violin bow and a string. Part iii: Parameter dependence," *Acta Acust. united Ac.*, **84**, 929–946 (1998).

[42] J. Smith and J. Woodhouse, "The tribology of rosin," *J. Mech. Phys. Solids*, **48**, 1633–1681 (2000).

[43] P. Galluzzo, J. Woodhouse and H. Mansour, "Assessing friction laws for simulating bowed-string motion," *Acta Acust. united Ac.*, **103**, 1080–1099 (2017).

[44] C. Desvages, "Physical modelling of the bowed string and applications to sound synthesis," *Ph.D. Thesis, The University of Edinburgh* (2018).

[45] S. Serafin, "The sound of friction: Real-time models, playability and musical applications," *Ph.D. Thesis, Stanford University* (2004).

[46] C. Issanchou, S. Bilbao, J.-L. Le Carrou, C. Touzé and O. Doaré, "A modal-based approach for the nonlinear vibration of strings against a unilateral obstacle: Simulations and experiments in the pointwise case," *J. Sound Vib.*, **393**, 229–251 (2017).

[47] H. Cabannes, "Cordes vibrantes avec obstacles (vibrating strings with obstacles)," *Acustica*, **55**, 14–20 (1984).

[48] S. Bilbao, A. Torin and V. Chatziioannou, "Numerical modeling of collisions in musical instruments," *Acta Acust. united Ac.*, **101**, 155–173 (2015).

[49] S. Bilbao and A. Torin, "Numerical modeling and sound synthesis for articulated string/fretboard interactions," *J. Audio Eng. Soc.*, **63**, 336–347 (2015).

[50] M. Ducceschi, S. Bilbao, S. Willemsen and S. Serafin, "Linearly-implicit schemes for collisions in musical acoustics based on energy quadratisation," *J. Acoust. Soc. Am.*, **149**, 3502–3516 (2021).

[51] G. Evangelista and F. Eckerholm, "Player instrument interaction models for digital waveguide synthesis of guitar: Touch and collisions," *IEEE Trans. Audio Speech Lang. Proces.*, **18**, 822–832 (2010).

[52] V. Debut and J. Antunes, "Physical synthesis of sixstring guitar plucks using the Udwadia-Kalaba modal formulation," *J. Acoust. Soc. Am.*, **148**, 575–587 (2020).

[53] R. Burridge, J. Kappraff and C. Morshedi, "The sitar string, a vibrating string with a one-sided inelastic constraint," *SIAM J. Appl. Math.*, **42**, 1231–1251 (1982).

[54] A. Alsahlani and R. Mukherjee, "Vibration of a string wrapping and unwrapping around an obstacle," *J. Sound Vib.*, **329**, 2707–2715 (2010).

[55] A. Mandal and P. Wahi, "Natural frequencies, modeshapes and modal interactions for strings vibrating against an obstacle: Relevance to sitar and veena," *J. Sound Vib.*, **338**, 42–59 (2015).

[56] G. Kirchhoff, *Vorlesungen über Mechanik* (Tauber, Leipzig, 1883).

[57] G. F. Carrier, "On the nonlinear vibration problem of the elastic string," *Q. Appl. Math.*, **3**, 157–165 (1945).

[58] D. Oplinger, "Frequency response of a nonlinear stretched

string," *J. Acoust. Soc. Am.*, **32**, 1529–1539 (1960).
[59] G. Anand, "Large-amplitude damped free vibration of a stretched string," *J. Acoust. Soc. Am.*, **45**, 1089–1096 (1968).
[60] R. Narasimha, "Nonlinear vibration of an elastic string," *J. Sound Vib.*, **8**, 134–146 (1968).
[61] O. O'Reilly and P. Holmes, "Non-linear, non-planar and non-periodic vibrations of a string," *J. Sound Vib.*, **153**, 413–435 (1992).
[62] P. Morse and U. Ingard, *Theoretical Acoustics* (Princeton University Press, Princeton, 1968).
[63] C. Vallette, "The mechanics of vibrating strings," in *Mechanics of Musical Instruments*, A. Hirschberg, J. Kergomard and G. Weinreich, Eds. (Springer, New York, 1995), pp. 116–183.
[64] R. Dickey, "Infinite systems of nonlinear oscillation equations related to the string," *Proc. Am. Math. Soc.*, **23**, 459–468 (1969).
[65] R. Dickey, "Stability of periodic solutions of the nonlinear string," *Q. Appl. Math.*, **38**, 253–259 (1980).
[66] C. Gough, "The nonlinear free vibration of a damped elastic string," *J. Acoust. Soc. Am.*, **75**, 1770–1776 (1984).
[67] K. Legge and N. Fletcher, "Nonlinear generation of missing modes on a vibrating string," *J. Acoust. Soc. Am.*, **76**, 5–12 (1984).
[68] V. Välimäki, T. Tolonen and M. Karjalainen, "Plucked-string synthesis algorithms with tension modulation nonlinearity," *Proc. IEEE Int. Conf. Acoust. Speech Signal Process. (ICASSP) 1999*, Vol. 2, pp. 977–980 (1999).
[69] T. Tolonen, V. Välimäki and M. Karjalainen, "Modelling of tension modulation nonlinearity in plucked strings," *IEEE Trans. Speech Audio Process.*, **8**, 300–310 (2000).
[70] S. Bilbao and J. O. Smith III, "Energy conserving finite difference schemes for nonlinear strings," *Acta Acust. united Ac.*, **91**, 299–311 (2005).
[71] H. Penttinen, C. Erkut, J. Pölkki, V. Välimäki and M. Karjalainen, "Design and analysis of a modified kantele with increased loudness," *Acta Acust. united Ac.*, **91**, 261–268 (2005).
[72] T. Hélie and D. Roze, "Sound synthesis of a nonlinear string using Volterra series," *J. Sound Vib.*, **314**, 275–306 (2008).
[73] H. Conklin, "Generation of partials due to nonlinear mixing in a stringed instrument," *J. Acoust. Soc. Am.*, **105**, 536–545 (1999).
[74] E. Rokni, L. Neldner, C. Adkison and T. Moore, "The production of phantom partials due to nonlinearities in the structural components of the piano," *J. Acoust. Soc. Am.*, **142**, EL344–EL349 (2017).
[75] B. Bank and L. Sujbert, "Generation of longitudinal vibrations in piano strings: From physics to sound synthesis," *J. Acoust. Soc. Am.*, **117**, 2268–2278 (2005).
[76] S. Bilbao, "Conservative numerical methods for nonlinear strings," *J. Acoust. Soc. Am.*, **118**, 3316–3327 (2005).
[77] J. Chabassier, A. Chaigne and P. Joly, "Modeling and simulation of a grand piano," *J. Acoust. Soc. Am.*, **134**, 648–665 (2013).
[78] M. Ducceschi and S. Bilbao, "Simulation of the geometrically exact nonlinear string via energy quadratisation," *J. Sound Vib.*, **534**, 117021 (2022).
[79] J. O. Smith III, "Efficient simulation of the reed-bore and bow-string mechanisms," *Proc. Int. Comput. Music Conf.*, The Hague, The Netherlands, pp. 275–280 (1986).
[80] K. Karplus and A. Strong, "Digital synthesis of plucked-string and drum timbres," *Comput. Music J.*, **7**(2), pp. 43–55 (1983).
[81] M. McIntyre, R. Schumacher and J. Woodhouse, "On the oscillations of musical instruments," *J. Acoust. Soc. Am.*, **74**, 1325–1345 (1983).
[82] M. Karjalainen, V. Välimäki and T. Tolonen, "Plucked-string synthesis: From the Karplus-Strong algorithm to digital waveguides and beyond," *Comput. Music J.*, **22**(3), pp. 17–32 (1998).
[83] B. Bank and V. Välimäki, "Robust loss filter design for digital waveguide synthesis of string tones," *IEEE Signal Proces. Lett.*, **10**, 18–20 (2003).
[84] E. Maestre, G. Scavone and J. O. Smith III, "Joint modeling of bridge admittance and body radiativity for efficient synthesis of string instrument sound by digital waveguides," *IEEE/ACM Trans. Audio Speech Lang. Process.*, **25**, 1128–1139 (2017).
[85] G. Cuzzucoli and V. Lombardo, "A physical model of the classical guitar, including the players touch," *Comput. Music J.*, **23**(2), pp. 52–69 (1999).
[86] M. Laurson, C. Erkut, V. Välimäki and M. Kuuskankare, "Methods for modeling realistic playing in acoustic guitar synthesis," *Comput. Music J.*, **25**(3), pp. 38–49 (2001).
[87] V. Välimäki, H. Penttinen, J. Knif, M. Laurson and C. Erkut, "Sound synthesis of the harpsichord using a computationally efficient physical model," *EURASIP J. Appl. Signal Process.*, **69**, 934–948 (2004).
[88] J. Rauhala, M. Laurson, H.-H. Lehtonen, V. Välimäki and V. Norilo, "A parametric piano synthesizer," *Comput. Music J.*, **32**(4), pp. 17–30 (2008).
[89] L. Gabrielli, V. Välimäki, H. Penttinen, S. Squartini and S. Bilbao, "A digital waveguide-based approach for Clavinet modeling and synthesis," *EURASIP J. Adv. Signal Process.*, **103**, pp. 2–14 (2013).
[90] J. D. Morrison and J.-M. Adrien, "Mosaic: A framework for modal synthesis," *Comput. Music J.*, **17**(1), pp. 45–56 (1993).
[91] G. Eckel, F. Iovino and R. Caussè, "Sound synthesis by physical modelling with modalys," *Proc. Int. Symp. Musical Acoustics*, Dourdan, France, pp. 479–482 (1995).
[92] M. Ducceschi and C. Touzé, "Modal approach for nonlinear vibrations of damped impacted plates: Application to sound synthesis of gongs and cymbals," *J. Sound Vib.*, **334**, 313–331 (2015).
[93] J. Strikwerda, *Finite Difference Schemes and Partial Differential Equations* (SIAM, Philadelphia, 2004).
[94] B. Gustaffson, H.-O. Kreiss and J. Oliger, *Time Dependent Problems and Difference Methods* (John Wiley & Sons, New York, 1996).
[95] R. Courant, K. Friedrichs and H. Lewy, "On the partial differential equations of mathematical physics," *Math. Ann.*, **100**, 32–74 (1928) (in German).
[96] M. Rubin and O. Gottlieb, "Numerical solutions of forced vibration and whirling of a nonlinear string using the theory of a Cosserat point," *J. Sound Vib.*, **197**, 85–101 (1996).
[97] A. Watzky, "Non-linear three-dimensional large-amplitude damped free vibration of a stiff elastic stretched string," *J. Sound Vib.*, **153**, 125–142 (1992).
[98] F. Gillan and S. Eliot, "Measurement of the torsional modes of vibration of the strings on instruments of the violin family," *J. Sound Vib.*, **130**, 347–351 (1989).
[99] E. Bavu, J. Smith and J. Wolfe, "Torsional waves in a bowed string," *Acta Acust. united Ac.*, **91**, 241–246 (2005).
[100] G. Weinreich, "Coupled piano strings," *J. Acoust. Soc. Am.*, **62**, 1474–1484 (1977).

Stefan Bilbao (B.A. Physics, Harvard, 1992, MSc., PhD Electrical Engineering, Stanford, 1996 and 2001 respectively) is currently Professor of Acoustics and Audio Signal Processing in the Acoustics and Audio Group at the University of Edinburgh, and previously held positions at the Sonic Arts Research Centre, at the Queen's University Belfast, and the Stanford Space Telecommunications and Radioscience Laboratory. He was born in Montreal, Quebec, Canada.

Michele Ducceschi (BSc. Physics (2008), University of Padova, Italy, MSc. Acoustics (2010), University of Edinburgh, UK, PhD Mechanical Engineering (2014), ENSTA and Ecole Polytechnique, France) is currently an Associate Professor at the University of Bologna in Italy. He is currently the P.I. of the ERC-funded project NEMUS (2021–2026). Previously, he held positions at the University of Edinburgh. He was a Royal Society Newton International Fellow, and a Leverhulme Early Career Fellow.